Applied Radiation and Isotopes 176 (2021) 109762

Contents lists available at ScienceDirect

Applied Radiation and Isotopes

journal homepage: www.elsevier.com/locate/apradiso

Optimization of alkali fusion process for determination of I-129 in solidified radwastes by neutron activation

Jiunn-Hsing Chao [a,*], Chun-Yu Chuang [b], Wei-Chun Chou [b,c], Chun-Liang Kuo [d], Feng-Chih Chang [e], An-Chung Chiang [a]

[a] Nuclear Science and Technology Development Center, National Tsing Hua University, Hsinchu, 30013, Taiwan, ROC
[b] Department of Biomedical Engineering and Environmental Sciences, National Tsing Hua University, Hsinchu, 30013, Taiwan, ROC
[c] Institute of Computational Comparative Medicine, Department of Anatomy and Physiology, College of Veterinary Medicine, Kansas State University, Manhattan, KS, United States
[d] Department of Nuclear Medicine, Hsinchu Mackay Memorial Hospital, Hsinchu, 30071, Taiwan, ROC
[e] Chemical Division, Institute of Nuclear Energy Research, Longtan, 32546, Taiwan, ROC

ARTICLE INFO

Keywords:
^{129}I
Radwaste
Alkali fusion
Neutron activation analysis

ABSTRACT

This study determines the optimum temperature for the alkali fusion process used to effectively separate iodine from solidified radwaste attaining low-level ^{129}I by neutron activation. The alkali fusion temperature was adjusted to 120, 200, and 400 °C to approach the optimum conditions associated with a good statistical distribution of the measured ^{129}I data and high chemical recovery yield. Statistical analysis revealed that the optimum temperature of the alkali fusion process was 200 °C, displaying good central tendency and low variance of the measured ^{129}I data, and the respective chemical recovery yields were higher than other temperatures. The optimum fusion condition provides more reliable scaling factors (^{129}I/^{137}Cs) of radwaste.

1. Introduction

Iodine-129 (^{129}I), which emits low-energy characteristic photons, is defined as an important difficult-to-measure (DTM) nuclide in radwaste (IAEA, 2009). ^{129}I is produced from the operation and decommissioning processes in nuclear power plants. Some studies predict that ^{129}I may accumulate in the terrestrial environment and reach the biosphere, contributing to long-term exposure (Grambow, 2008; Kocher, 1991). Activity concentrations of ^{129}I or the derived scaling factors of ^{129}I/^{137}Cs in radwaste should be determined before the classification of low-level radwaste and final disposal design (NRC, 1982). Generally, radiochemical separation of ^{129}I from solid samples, such as soils and cemented radwaste, is necessary before instrumental measurements. Separation techniques, such as volatilization (Muramatsu et al., 1985; Remenec et al., 2017), chemical distillation (Martin et al., 1990), and alkali fusion (Chao et al., 1999; Kuo et al., 2013; Osterc et al., 2007), which are followed by neutron activation and/or radiometric measurements, are commonly used to separate and analyze iodine ^{129}I in soil and solidified radwaste samples. The function of alkali fusion is to decompose all organic matter, which may physically and/or chemically fix iodine (and ^{129}I), allowing it to be released as iodide for subsequent separation by solvent extraction.

The matrices of cement-solidified radwaste are complicated because of the various origins of radioactive waste generated in nuclear facilities. Besides, most radwaste contain a variety of radionuclides with high activities, these are not suitable to be treated with high-temperature separation processes, such as volatilization and combustion, which could easily result in radioactive contaminations during chemical separation. Alkali fusion processes at relatively low temperatures may be the best choice. Almost no literature deals with the adequate temperature of alkali fusion for solidified radwaste. A previous study determined the ^{129}I activity in cement-solidified radwaste by alkali fusion followed by solvent extraction to separate iodine (and ^{129}I) before neutron activation; the fusion temperature was set at 400 °C and the chemical recovery yield was 30–50% (Kuo et al., 2013), which may be modified by varying the fusion temperature to improve the separation effectiveness and chemical yield. In this study, the fusion temperature was adjusted from 120 to 400 °C to determine the optimum fusion conditions. Radwaste samples were alkali-fused using KOH, and then ^{129}I and iodine carrier (KI) were chemically separated by solvent extraction before and after neutron irradiation. The activated products of stable iodine (^{127}I) and ^{129}I were measured using a gamma-ray spectrometer. The ^{129}I

* Corresponding author.
E-mail address: jhchao@mx.nthu.edu.tw (J.-H. Chao).

https://doi.org/10.1016/j.apradiso.2021.109762
Received 4 January 2021; Received in revised form 25 March 2021; Accepted 27 April 2021
Available online 29 May 2021

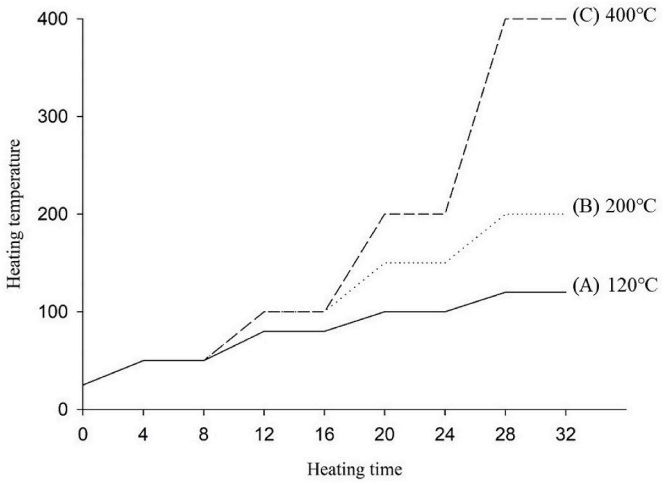

Fig. 1. Temperature raising program for the alkaline fusion process: A (120 °C), B (200 °C), and C (400 °C).

activity in the test samples was determined and the measured data were statistically analyzed to determine the optimum fusion condition based on their activity distribution and variance. In addition, the chemical recovery yields associated with the sample separation processes were used to explain the separation effectiveness of the three fusion processes. In contrast, scaling factors ($^{129}I/^{137}Cs$) were evaluated based on the ^{129}I activities determined using the optimum fusion condition.

2. Materials and methods

2.1. Sample preparation

A total of 15 cement-solidified radioactive waste samples were treated using various alkali fusion conditions to separate iodine (and ^{129}I) before solvent extraction and neutron activation. The wastes, including radioactive sludge, concentrates, and/or resins, were produced during the decommissioning of nuclear facilities of the Institute of Nuclear Energy Research (INER) (Chou and Fan, 2006; Wei et al., 2009) and solidified by cement to form various crystalline matrices. The samples were crushed and ground into a fine powder using a mortar before alkali fusion. Before alkali fusion, gamma-ray emitters, such as ^{137}Cs, in these samples were determined using a gamma-ray spectrometer, as described in Section 2.5.

2.2. Alkali fusion process

Powdered radwaste samples (1 g) and KOH (4 g) were mixed in a 50-mL nickel crucible, and a 1 mL carrier solution containing 20 mg KI was added as a carrier to evaluate the chemical recovery yield during the purification process. The crucible was placed in a furnace, and fusion processes were programmed and raised from room temperature to 120 °C (process A), 200 °C (process B), and 400 °C (process C). Fig. 1 illustrates the temperature raising program for the fusion process.

2.3. Solvent extraction

After completing the alkali fusion, the residue was neutralized, resolved with diluted HNO_3, and then transferred to a separating funnel containing 40 mL of n-hexane. Both iodide (I^-) and iodate (IO_3^-) can be converted to iodine (I_2) by adding $NaNO_2$, and iodine is extracted into the organic phase. The organic phase was washed twice with deionized water, and the aqueous phase containing various mineral impurities was discarded to avoid unwanted interfering radionuclides in the subsequent gamma-ray measurements. Reducing iodine (I_2) into iodide (I^-) by adding H_2SO_3 and iodide was back-extracted into the aqueous phase. The iodide was precipitated as MgI_2 by adding MgO powder to the aqueous solution.

2.4. Neutron activation

The prepared MgI_2 was enclosed in a 1-mL vial for neutron irradiation for 2 h by using the Tsing Hua Open-pool Reactor (THOR), where neutron fluence rate of 10^{12} cm^{-2} s^{-1}. A comparative standard containing 1 mL of the carrier solution and 0.08 Bq ^{129}I (a known atomic ratio of $^{129}I/^{127}I = 8.0 \times 10^{-7}$) was also activated in parallel with the test samples. After 20 h of cooling, the iodine (and ^{129}I) in the test samples and the standard were separated again by solvent extraction, as described in Section 2.3. The final concentrated solution (10 mL) was used for the determination of iodine (^{127}I) and ^{129}I by gamma-ray measurements.

2.5. Radioactivity measurement

The solution was measured using a high-purity germanium detector (GC3020, Canberra Meriden, Connecticut, USA) coupled with a multichannel analyzer and a software package (Genie, 2000; Canberra). Both stable iodine (^{127}I) and ^{129}I are activated by neutrons through ^{127}I (n, 2n) ^{126}I and ^{129}I (n,γ) ^{130}I reactions; their activated radionuclides were measured simultaneously with a high-purity germanium-based gamma-ray spectrometer. The activity of ^{130}I was determined based on its characteristic gamma energies of 536 and 740 keV, while the activity of ^{126}I was determined according to its characteristic gamma energy of 389 keV.

2.6. Determination of ^{129}I activity and associated minimum detectable amount (MDA)

Because the waste samples and the standard were irradiated together by neutrons, the $^{129}I/^{127}I$ and ^{129}I activities in the samples were calculated as follows:

$$\frac{\left(^{129}I/^{127}I\right)_{sa}}{\left(^{129}I/^{127}I\right)_{st}} = \frac{(A130/A126)_{sa}}{(A130/A126)_{st}}, \quad [1]$$

where A_{130} denotes the activity of ^{130}I and ^{126}I denotes that of ^{126}I. Therefore,

$$^{129}Isa = \frac{(A130/A126)_{sa}}{(A130/A126)_{st}} \times {}^{129}Ist, \quad [2]$$

where 129Ist = 0.08 Bq.

The MDA associated with ^{129}I determination is based on the following definition (Currie, 1968):

$$MDA\left(^{130}I\right) = \frac{4.65\sqrt{B} + 2.71}{\varepsilon \times t \times m}, \quad [3]$$

where B denotes the spectral background (counts) under the characteristic gamma rays for the ^{130}I measurement, ε denotes the detection efficiency of the gamma energy, t is the counting duration, and m is the sample weight (1 g).

2.7. Statistical analysis

Statistical analysis was conducted using SPSS 20.0, and all statistical significance was determined with a two-tailed $p < 0.05$. Data presented as geometric means (GM) ± geometric standard deviation (SD) were calculated as follows:

$$GM = \sqrt[n]{\prod_{i=1}^{n} X_i} = \sqrt[n]{x_1 . x_2 \ldots x_n}, \quad [4]$$

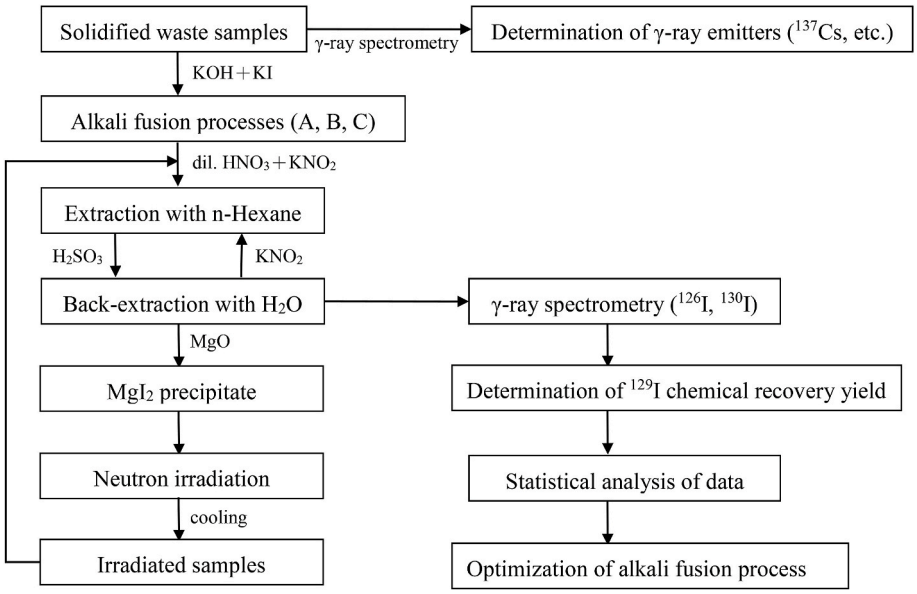

Fig. 2. Schematic diagram of the chemical separation, radioactivity determination, and statistical analysis to determine the fusion optimum temperature.

and

$$SD = \exp\left(\sqrt{\frac{\sum_{i=1}^{n}\left(\left(\ln\frac{x_i}{GM}\right)^2\right)}{n}}\right), \quad [5]$$

where X denotes the values of the measurement and n is the total number of samples.

One-way ANOVA test used to determine the differences between three or more groups was calculated as follows:

$$y_{ij} = m + a_i + \varepsilon_{ij}. \quad [6]$$

The equation indicates that the jth data value, from level i, is the sum of three components: the grand mean (m), the deviation of each value from the grand mean (a), and the residual (ε).

The central tendency and dispersion for normality were evaluated using the Kolmogorov-Smirnov test on activity concentration of ^{129}I of the test samples through alkali fusion processes with temperatures of 120, 200, and 400 °C. Kolmogorov-Smirnov tests were performed to test the hypothesis that the distributional form rejected if the test statistic (D) was greater than the critical value. The data of each variable (Y) follow a Gaussian distribution, where F is the theoretical cumulative distribution of the distribution being tested, which must be continuous.

$$D = \max_{1\le i\le n}\left(F(Y_i) - \frac{i-1}{n}, \frac{i}{n} - F(Y_i)\right) \quad [7]$$

Additionally, the cumulative distribution function (CDF) of chemical recovery yield (%) was generated by Monte Carlo (MC) simulation (Cook and DelRio, 2019; Wei and Zhang, 2018) using the R functions "rlnorm" and "ecdf" in R language (version 3.5.2, 2018; R Development Core Team, http://www.R-project.org). The CDF of a continuous random variable x is estimated as follows:

$$F(x) = \int_{-\infty}^{x} f(y)dy, \quad [8]$$

where CDF denotes as "$F(x)$" that expresses the integral of the probability density function ($f(y)$) of chemical recovery yield (y).

Table 1
Activity (A) and recovery yield (Y) for analysis of ^{129}I in radwaste samples through various alkali fusion temperatures.

Radwaste Sample	120 °C		200 °C		400 °C		p-value
	A (Bq/g)	Y (%)	A (Bq/g)	Y (%)	A (Bq/g)	Y (%)	
1	2.7 ± 0.4	39	2.2 ± 0.3	66	2.1 ± 0.2	59	0.113
2	2.9 ± 0.3	57	2.1 ± 0.4	51	2.3 ± 0.3	45	0.062
3	4.7 ± 0.4	17	3.1 ± 0.4	33	2.1 ± 0.5	7.5	0.001*
4	0.67 ± 0.15	72	0.46 ± 0.16	69	<0.42	47	–
5	3.5 ± 0.6	31	1.8 ± 0.3	80	3.2 ± 0.3	49	0.006*
6	30 ± 3.0	32	30 ± 3.0	50	34 ± 3.0	34	0.248
7	1.4 ± 0.3	59	2.8 ± 0.3	67	2.2 ± 0.2	64	0.002*
8	0.50 ± 0.15	62	0.99 ± 0.17	61	0.94 ± 0.19	57	0.023*
9	3.6 ± 0.5	49	2.8 ± 0.3	100	2.2 ± 0.3	53	0.011*
10	4.1 ± 0.5	58	4.2 ± 0.5	49	3.4 ± 0.4	20	0.154
11	7.5 ± 1.0	15	3.7 ± 0.4	91	3.6 ± 0.5	34	0.001*
12	<1.5	19	<0.52	100	<0.38	44	–
13	0.61 ± 0.16	63	<0.52	64	<1.4	18	–
14	1.8 ± 0.3	52	1.8 ± 0.4	35	<9.7	2.0	–
15	<4.4	77	7.8 ± 0.8	87	11 ± 1.0	12	–
Geometric Mean	2.6	41.7	2.2	63.5	2.6	27.5	
Geometric SD	2.8	1.7	2.8	1.4	3.1	2.6	
Variance	61	404	60	459	93	400	

Note: (1) The activity of the sample was used as its MDA value if its activity was lower than that of MDA; (2) * indicates $p < 0.05$.

(a)

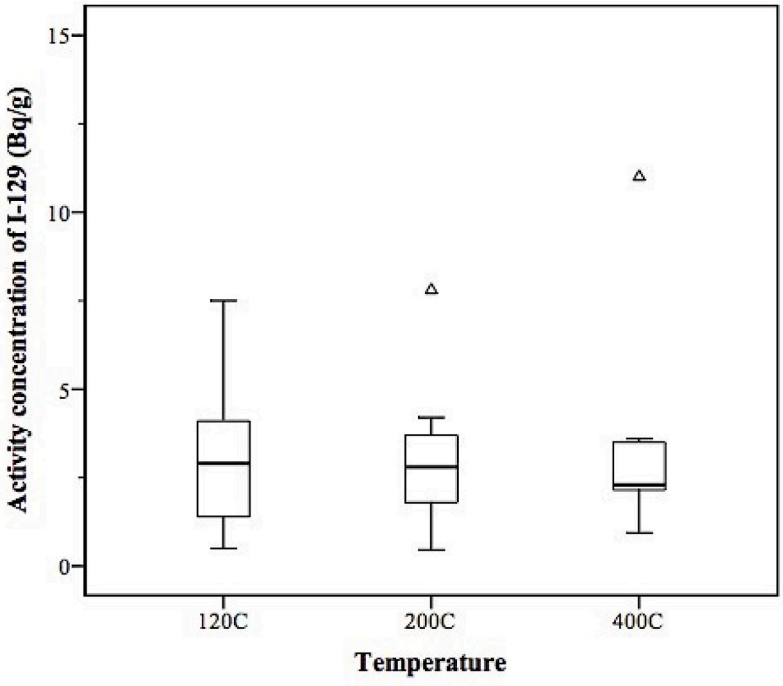

(b) Normal Q-Q plot of ^{129}I activity

Raw data

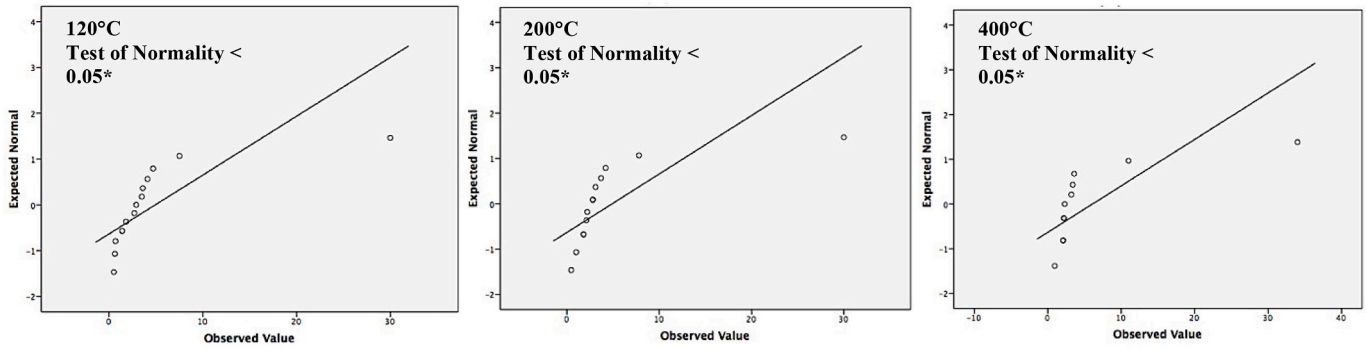

After log transformation

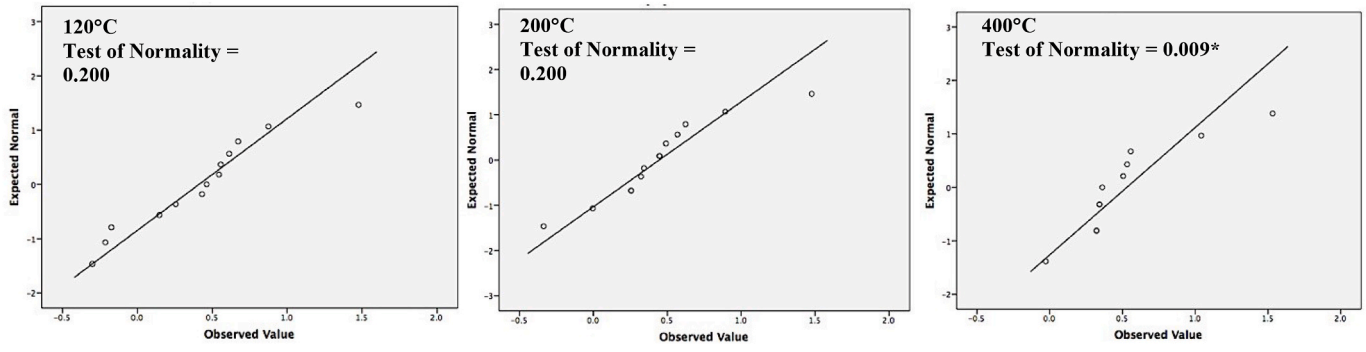

Fig. 3. Confirmation of the central tendency distribution of ^{129}I activity concentrations at various alkaline fusion temperatures. (a) The boxplot showed the variation and (b) the Q-Q plot presented the normality situation, respectively, for the distribution of ^{129}I activity concentrations in 15 radwaste samples determined at 120 °C, 200 °C, and 400 °C.

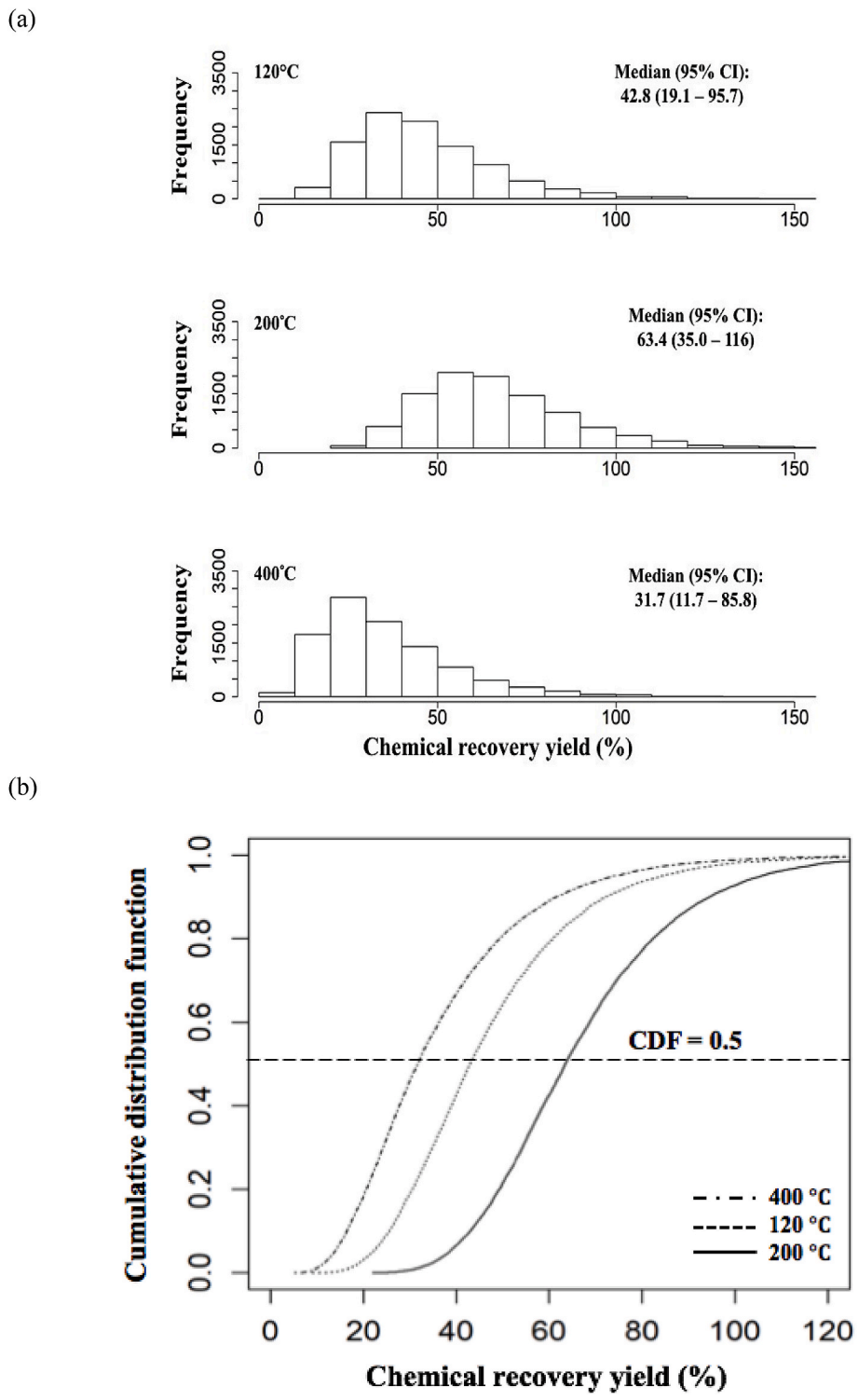

Fig. 4. Monte Carlo simulation for estimating the yield of ^{129}I activity determination at various alkaline fusion temperatures. (a) The Monte Carlo algorithm was displayed to stimulate the recovery yields in 3500 frequencies, and (b) the cumulative distribution function curve was illustrated versus recovery yield percentages of Monte Carlo simulation at 120 °C, 200 °C, and 400 °C, respectively.

2.8. Evaluation of scaling factor

The scaling factors (^{129}I/^{137}Cs) of the radwaste samples were evaluated based on the measured ^{129}I activities determined using the optimum fusion condition.

Fig. 2 is a schematic diagram of the separation/analysis process and the subsequent statistical analysis for the determination of the optimum alkali fusion temperature.

3. Results and discussion

3.1. Measured ^{129}I activity and chemical recovery yield

The activity concentrations of ^{129}I and the respective chemical

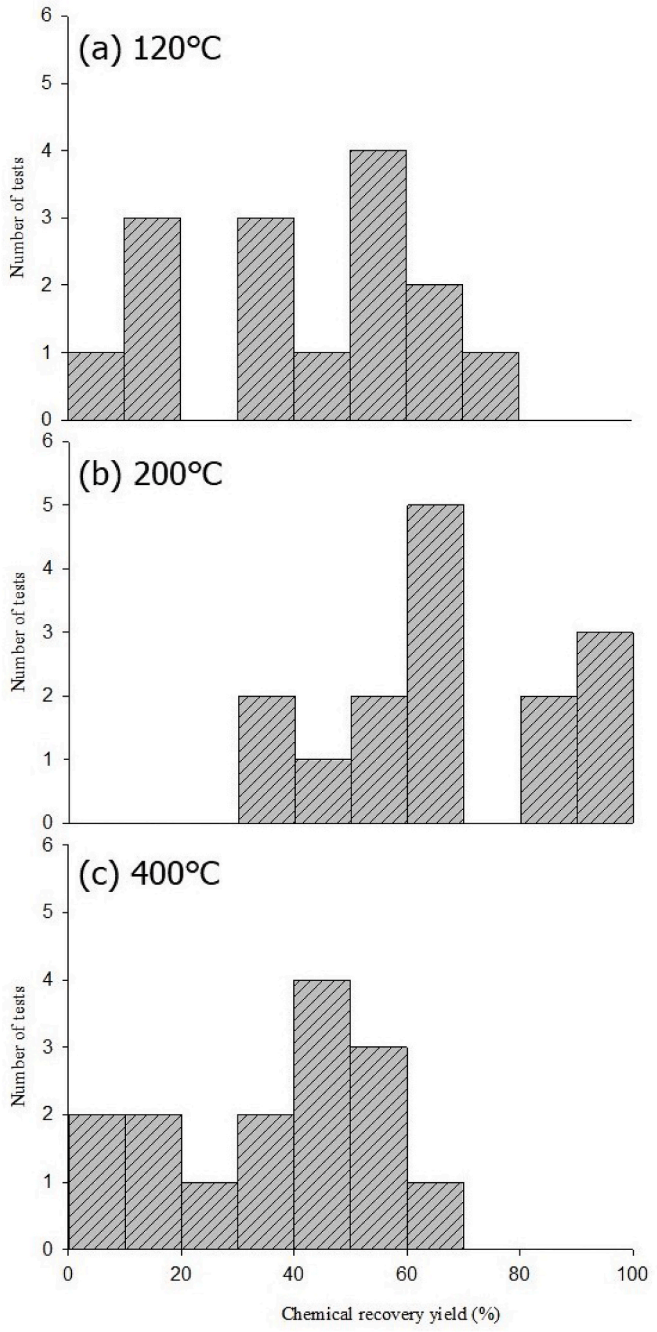

Fig. 5. The range of chemical recovery yield (%) of iodine for ^{129}I determination by neutron activation at various fusion temperatures: (a) 120 °C, (b) 200 °C, and (c) 400 °C.

recovery yields of the 15 samples through the three different fusion processes are listed in Table 1. The p-values imply consistency among the measured data across the three fusion temperatures; $p < 0.05$ indicates a significant difference between the fusion processes on the separation/recovery results. The GM, SD, and variance associated with the measured ^{129}I for the 15 samples in the three fusion processes are also indicated.

3.2. Optimum alkali fusion temperature for ^{129}I determination

To determine the optimum alkali fusion temperature for ^{129}I determination, a boxplot was plotted according to the measured ^{129}I activity concentrations in the 15 radwaste samples at 120 °C, 200 °C, and 400 °C,

Table 2
The scaling factor (SF) of ^{129}I/^{137}Cs evaluated based on the activity of ^{129}I determined through the optimum fusion temperature (200 °C).

Radwaste Sample	137Cs activity (Bq/g)	SF (129I/137Cs)
1	$(6.18 \pm 0.08) \times 10^3$	$(3.6 \pm 0.5) \times 10^{-4}$
2	$(3.57 \pm 0.05) \times 10^3$	$(5.9 \pm 1.1) \times 10^{-4}$
3	$(1.91 \pm 0.02) \times 10^3$	$(16 \pm 2) \times 10^{-4}$
4	$(5.10 \pm 0.07) \times 10^3$	$(0.9 \pm 0.3) \times 10^{-4}$
5	$(4.45 \pm 0.06) \times 10^3$	$(4.0 \pm 0.7) \times 10^{-4}$
6	$(7.05 \pm 0.09) \times 10^3$	$(43 \pm 4) \times 10^{-4}$
7	$(1.71 \pm 0.02) \times 10^3$	$(16 \pm 2) \times 10^{-4}$
8	$(5.04 \pm 0.07) \times 10^3$	$(2.0 \pm 0.3) \times 10^{-4}$
9	$(3.45 \pm 0.05) \times 10^3$	$(8.1 \pm 1.0) \times 10^{-4}$
10	$(6.09 \pm 0.08) \times 10^3$	$(6.9 \pm 0.8) \times 10^{-4}$
11	$(6.47 \pm 0.09) \times 10^3$	$(5.7 \pm 0.6) \times 10^{-4}$
12	$(1.33 \pm 0.01) \times 10^3$	$<3.9 \times 10^{-4}$
13	$(4.28 \pm 0.06) \times 10^3$	$<1.2 \times 10^{-4}$
14	$(2.23 \pm 0.03) \times 10^3$	$(8.1 \pm 1.8) \times 10^{-4}$
15	$(4.73 \pm 0.06) \times 10^3$	$(16 \pm 2) \times 10^{-4}$
Geometric Mean		5.9×10^{-4}

Note: The SF of the sample was used as its MDA value if its ^{129}I activity was lower than that of MDA.

and showed that the distribution of ^{129}I activity concentrations at 200 °C was fit to the central tendency very well and the dispersion was small (Fig. 3a). We further statistically tested their normality using the Kolmogorov-Smirnov test (Fig. 3b), showing that the observed values of ^{129}I activity concentrations at 120 °C ($p = 0.200$) and at 200 °C ($p = 0.200$) individually fit the line consisting of expected values after logarithmic conversion, which indicated that the concentrations of ^{129}I activity determined at 120 °C and 200 °C presented a normal distribution. Additionally, the values of variance at 200 °C were lower than those at 120 °C and 400 °C (Table 1).

3.3. Chemical recovery yield

According to the chemical yields listed in Table 1, more samples were effectively recovered during the 200 °C analysis process (Fig. 4a), and over 50% of the samples exceeded the yield ratios more than 60% at 200 °C (23% at 400 °C and 33% at 120 °C) in CDF curves (Fig. 4b). Fig. 5 illustrates the distribution of chemical recovery yields for the three fusion processes, where the highest recovery yield (on average) is found in process B (200 °C). During alkali fusion and chemical separation processes, we observed that the alkali-fused samples were almost completely resolved by nitric acid to a clear solution in process B, while insoluble remains were occasionally seen in Processes A and C. These results suggest that an alkali fusion temperature of 200 °C is optimal for the separation and analysis of ^{129}I activity concentrations for these solidified radwaste samples.

3.4. Scaling factor (SF) of ^{129}I/^{137}Cs

Based on the ^{129}I activity concentrations determined using the optimum fusion condition (200 °C) and the respective ^{137}Cs activities for the 15 radwaste samples, the GM of ^{129}I/^{137}Cs was calculated to be 5.9×10^{-4} (Table 2), providing a reliable relationship between ^{129}I and ^{137}Cs.

4. Conclusions

Based on the statistical analysis of the measured ^{129}I data of the 15 radwaste samples, the optimum temperature for the alkali fusion process for the separation of iodine was determined to be 200 °C. Besides, chemical recovery yield in the temperature (200 °C) was 64% on average, relatively higher than those of 120 °C (42%) and 400 °C (28%). The optimum fusion temperature (Process B) provides good separation performance with a higher chemical recovery yield, which results in a

corresponding lower detection limit. Accordingly, the optimum fusion process can be applied to the determination of low-level ^{129}I activity and the associated SF ($^{129}I/^{137}Cs$) for the solidified radwaste, which can be applied to the classification of radwaste for final disposal.

Declaration of competing interest

The authors declare that they have no known competing financial interests or personal relationships that could have appeared to influence the work reported in this paper.

Acknowledgments

This work was financially supported by the Ministry of Science and Technology of the Republic of China (Taiwan) under Contract No. MOST 108-2221-E−007-047.

References

Chao, J.H., Tseng, C.L., Lee, C.J., Hsia, C.C., Teng, S.P., 1999. Analysis of I-129 in radwastes by neutron activation. Appl. Radiat. Isot. 51, 137–143.

Chou, I.H., Fan, C.F., 2006. Developing Integrated decommissioning information management system (IDIMS) of nuclear facilities. J. Nucl. Sci. Technol. 43, 596–604.

Cook, R.F., DelRio, F.W., 2019. Material flaw populations and component strength distributions in the context of the Weibull Function. Exp. Mech. 59, 279–293.

Currie, L.A., 1968. Limits for qualitative detection and qualitative determination and quantitative determination. Application to radiochemistry. Anal. Chem. 40, 586–593.

Grambow, B., 2008. Mobile fission and activation products in nuclear waste disposal. J. Contam. Hydrol. 102, 180–186.

International Atomic Energy Agency (IAEA), 2009. Determination and Use of Scaling Factors for Waste Characterization in Nuclear Power Plants. Nuclear Energy Series No. NW-T-1.18, Vienna.

Kocher, D.C., 1991. A validation test of a model for long-term retention of I-129 in surface soils. Health Phys. 60, 523–531.

Kuo, C.L., Tsai, T.L., Chiang, A.C., Chang-Liao, K.S., Chao, J.H., 2013. Determination of ^{129}I in cement-solidified radwastes using neutron activation. J. Radioanal. Nucl. Chem. 298, 465–473.

Martin, J.E., Marciowski, F., Cook, S.K., 1990. Optimization of neutron activation of ^{129}I in low-level radioactive waste samples. Appl. Radiat. Isot. 41, 727–731.

Muramatsu, Y., Uchida, S., Sumiya, M., Ohmomo, Y., 1985. Iodine separation procedure for the determination of ^{129}I and ^{127}I in soil by neutron activation analysis. J. Radioanal. Nucl. Chem. Lett. 94, 329–338.

Nuclear Regulatory Commission (NRC), 1982. Licensing Requirements for Land Disposal of Radioactive Waste. Code of Federal Regulations, 10CFR61. Office of Federal Register, Washington D. C.

Osterc, A., Jacimovic, R., Stibilj, V., 2007. Development of a method for ^{129}I determination using radiochemical neutron activation analysis. Acta Chim. Slov. 54, 273–283.

Remenec, B., Dulanská, S., Horváthová, B., Mátel, Ľ., 2017. Determination of ^{129}I using volatilization method and liquid scintillation spectrometry. J. Radioanal. Nucl. Chem. 311, 1649–1655.

Wei, M., Zhang, L., 2018. Application of distribution functions in accurate determination of interdiffusion coefficients. Sci. Rep. 8, 5071.

Wei, H.J., Tsai, T.L., Wang, J.J., Chen, I.J., Wuu, J.L., Wang, T.W., 2009. Clearance measurement of metal scraps for nuclear facility at INER in Taiwan. Appl. Radiat. Isot. 67, 944–949.